

MSAT BOOM JOINT TESTING AND LOAD ABSORBER DESIGN

D.H. Klinker, K. Shuey, and D.R. St. Clair
Lockheed Missiles and Space Co.
Sunnyvale, California

ABSTRACT

Through a series of component and system-level tests, the torque margin for the MSAT booms is being determined. The verification process has yielded a number of results and lessons that can be applied to many other types of deployable spacecraft mechanisms.

The MSAT Load Absorber has proven to be an effective way to provide high energy dissipation using crushable honeycomb. Using two stages of crushable honeycomb and a fusible link, a complex crush load profile has been designed and implemented. The design features of the Load Absorber lend themselves to use in other spacecraft applications.

INTRODUCTION

MSAT is a commercial project developing a satellite-based cellular telephone, data, and fax network that will provide coverage throughout North America. When the system is fully operational, MSAT will have two satellites, each having two large Wrap-Rib™ reflectors used to transmit and receive data. The reflectors are positioned on the satellites by graphite epoxy booms as shown in Figure 1. The MSAT booms offer a number of lessons and design solutions that can be applied to many types of deployable spacecraft mechanisms. This paper will provide an overall description of the MSAT booms and focus on two specific aspects: torque margin verification testing, and design and testing of an energy dissipating mechanism.

SECTION 1: BOOM DESCRIPTION

MSAT Wrap-Rib™ reflectors, designed and manufactured by Lockheed Missiles and Space Co. (LMSC), will be used to transmit and receive communications data on the MSAT satellites. The reflectors are parabolic with a maximum distance from rib tip to rib tip of 5.7 meters. Each reflector consists of a reflective mesh material supported by 16 flexible aluminum ribs attached to a 81-cm-diameter hub. The ribs are designed such that they can be tightly wound around the hub when the reflector is stowed. During deployment the ribs unwind to form a parabolic shape.

The reflectors are supported on the the spacecraft by graphite epoxy booms. Each boom has three joints ("Shoulder", "Elbow", and "Wrist"), connecting three graphite epoxy tubes, with a "Load Absorber" and "Reflector Positioning Mechanism" (RPM) at the end of the boom (See Figure 1). The Load Absorber is

used to dissipate energy from the reflector deployment and reduce the loads on the boom and spacecraft. The RPM (provided by Hughes Space and Communications) is used to provide fine pointing adjustments.

All three of the boom joints have essentially the same mechanism components: an eddy-current damper, two constant-torque laminated springs, two sets of duplex-pair angular-contact bearings, and a latch. Figure 2 shows the typical cross-section of each joint. The size and shape of each joint is different (see Figure 3), however they all share a common mechanism core.

The Load Absorber mechanism is shown in Figure 4. When the reflector ribs "lock-up", the Load Absorber interface plate rotates about the Load Absorber bearings. As it rotates, honeycomb in the Load Absorber Megatube is crushed, limiting the torque applied by the reflector and absorbing some of the energy of the deployment. Two stages of honeycomb are used in order to give two levels of crush force. After the honeycomb has been crushed and rotation about the Load Absorber bearing is stopped, the Load Absorber spring returns the Load Absorber interface plate back to its original position.

Over 95% of all boom surfaces are shielded from Passive Intermodulation (PIM) by PIM blankets, which also provide thermal protection. PIM is an electromagnetic phenomenon that is caused by energy being radiated off of PIM sources and interfering with incoming signals. PIM sources include such things as junctions of dissimilar metals, bolted interfaces, sharp corners, etc. The PIM shields have become quite complex and produce significant drag during deployment.

Power to the RPM is provided by a command and telemetry cable that runs the length of the boom. Also running the length of the boom are two pyro harnesses used to fire pinpullers at the joints and the reflector release mechanism. All of these harnesses cross the joints and Load Absorber producing significant drag at low temperatures.

SECTION 2: JOINT TORQUE MARGIN VERIFICATION

This next section will focus on the MSAT boom mechanism testing used in the torque margin verification process. Torque margin testing of the MSAT Reflector Boom joints produced a number insights on what tests should be performed on mechanisms and how to improve the efficiency of mechanisms testing. This section will give an outline of the torque margin verification method, a description of each component test, and present highlights from the test results.

TORQUE MARGIN DEFINITION

Torque margin is calculated using the following formula:

Torque Margin =	$\frac{\text{Deploying Torque} - \text{Dynamic Torque}}{\text{Resistive Torque}}$	= 1
-----------------	---	-----

For the boom joints, "Deploying Torque" is provided by the two constant-torque laminated springs. "Resistive Torques" are from harness bending, blanket bending, bearing friction, latching friction as well as less obvious sources such as spring losses due to interlaminar friction, and damper drag due to internal gear friction within the dampers. "Dynamic Torque" is resistance to deployment caused by spinning of the spacecraft. Due to the relatively low spin rate of the MSAT spacecraft during deployment (1 rpm), the dynamic torque does not significantly affect torque margin.

TEST PLAN

Torque margin verification testing was divided into three phases. Phase 1 involved testing the components that went into the joints separately prior to installation in the joints. Phase 2 involved testing the assembled joints prior to being bonded with the graphite epoxy tubes and Phase 3 tests are currently being performed on the assembled booms. Table 1 shows which parameters were measured during each phase of testing.

Table 1
Torque Margin Test Plan

	Phase 1 (Component)	Phase 2 (Joints)	Phase 3 (Booms)
Spring Torque	Ambient	Ambient	
Spring Friction	Ambient	Ambient	
Damper Drag	Ambient Cold Temp		
Damping Rate	Ambient Cold Temp		
Latch Friction (Protoflight only)		Ambient	Ambient (Hot & Cold Vac.)
Bearing Friction (Protoflight only)		Ambient	Ambient (Hot & Cold Vac.)
Harness Bending Torque (Protoflight only)			Ambient (Hot & Cold Vac.)
Blanket Bending Torque (Protoflight only)			Ambient (Hot & Cold Vac.)

As shown in Table 1, the spring torques and frictions are not measured at high or low temperatures. This was done primarily to save on testing time but also because it was assumed that no significant changes in the spring torque or the spring friction are likely to occur over the protoflight temperature range of -22°C to $+46^{\circ}\text{C}$. The springs are stainless steel that have stiffness properties that do not change significantly at the MSAT protoflight temperatures, making it unlikely that the torque available will change significantly. The properties of the dry-film lubrication used on the springs also do not change significantly at the protoflight temperatures.

Early on in the program, testing of the joints was given high priority by the design team. Designers working on the test equipment worked closely with the mechanisms designers to assure that the joints could be tested thoroughly and efficiently. Strong emphasis was placed on automating testing as much as possible in order to speed up the testing of all twelve joints. Most of the component and joint tests were run with motor-driven fixtures controlled by the same computer used for data acquisition. A Macintosh-based data acquisition program called LabView¹ provided flexible data acquisition options with very little programming time. Test fixtures were designed specifically for the MSAT joints making it very easy to set up and conduct tests. While these steps required a sizeable initial investment, they proved to provide significant reductions in testing time.

PHASE 1: COMPONENT TESTING

Spring Torque and Friction Tests

All of the joint deployment springs were component tested at ambient conditions by mounting them on a motor-driven fixture that cycled the springs three times and plotted the torque vs. angle hysteresis loops as shown in Figure 5. The torque available from the spring is the average between the stowing and deploying torques and the spring friction is half the difference between the stowing and deploying torques.

Springs were ordered with 6, 7, and 8 laminates in order to provide a range of torques from which to choose from. After all the springs were tested, the combination of springs that provided the desired torque was selected. For example, at the elbow one 7-laminate spring and one 8-laminate spring are used, while at the shoulder and wrist two 8-laminate springs are used. Having the flexibility to change torques by simply changing springs proved to be very valuable when additional torque was required in the development program.

Damper Component Testing

Each joint has an eddy-current damper installed along the axis of the joint as shown in Figure 2. The principles of the Honeywell-built eddy-current dampers are discussed in some detail in Reference 1. Basically, an eddy-current damper

¹ LABView, National Instruments Inc.

consists of a copper disk spinning between samarian-cobalt magnets, and a 4-stage planetary gear train. The damping rate at room temperature can be varied from 1100 N-m-s/rad to 2200 N-m-s/rad, by rotating a plate on the back of the damper that changes the alignment of the magnets.

Extensive component tests were run on each eddy-current damper to determine damper drag and damping rate over temperature. Damper drag is defined as the minimum torque necessary to cause the damper to rotate 360° without stopping.

Damper drag was tested to be on the order of 4.5 to 5.6 N-m, which was one of the primary sources of resistance in the joints. This was an important factor in the torque margin calculation because the damper friction largely drove the spring requirements, which in turn drove the damping requirements. In other words, selection of the eddy-current damper led to the requirement for larger springs, which led to the requirement for higher damping rates to accommodate the larger springs. Unfortunately, the higher damping rate and spring torques led to higher loads on the damper which is limited to 79.1 N-m. Meeting all the requirements required very careful balancing of these factors.

Damping rate was determined by applying a known torque on the damper and measuring the rotation vs. time. Figure 6 shows how the damping rates over temperature varied for two different dampers. Tests run over temperature demonstrated that damping rates vary widely from damper to damper. The temperature variation for each damper is most likely caused by changes in lubrication fluid viscosities, and changes in internal tolerances of the dampers at low temperatures. The variation in damping rate between different dampers is most likely caused by manufacturing tolerances.

Note, most of the testing done on the dampers over temperature was done to satisfy a requirement for simultaneity of the boom deployments. This requirement was canceled after the testing was complete, making most of the testing unnecessary. While the information obtained during these tests is interesting, it would have been much more economical to test at only the minimum, maximum, and room temperature, rather than over the range of temperatures.

Cable Harness Bending Tests

As part of the development test program, harness bending torques were measured at ambient and cold temperatures. The information gained from these tests helped in sizing of the deployment springs as well as being used in the final torque margin verification. Harness bending torque is the third largest cause of resistance after damper drag and spring friction.

PHASE 2: JOINT COMPONENT TESTING

Most of the extensive joint tests were run on the joint test stand shown in Figure 7. The joint test stand uses a stepper motor to open and close the joints, while load cells and a potentiometer monitor torque and angle. The stand also has an inertial simulator which approximates the inertial load the joints will see during deployment on the spacecraft. The inertial simulator consists of a bar with weights on the ends connected to the joint through a 20:1 gear box. The 20:1 gear box magnifies the effective inertia of the bar and weights by a factor of 20 squared.

Cold tests were run on the joint test stand by enclosing the inner portion of the stand with foam and spraying liquid and gaseous nitrogen into the enclosed region. The joint test stand proved to be extremely valuable by allowing the joints to be thoroughly tested before installation with the boom tubes, both at room temperature and cold temperature.

The first tests run on the joint test stand were bearing and latch friction tests. During these tests, the joints were opened and closed with no springs or damper installed. The primary purpose of these tests was to determine the latching torque and detect any problems with the bearings. The bearing torque was measured during these test to determine if the correct preload was on the bearings, and to determine if there was excessive drag on the bearings.

Next, the springs were installed and the joints were cycled with the springs to determine spring torque, and spring and bearing friction. Torque curves similar to Figure 5 were obtained, however, during these tests both springs were tested together and the friction value included friction from the fully loaded bearings. The torque information from these tests was used directly in the torque margin calculation as "Deploying Torque".

The last step in the joint acceptance sequence was to install the damper and run a series of deployment tests at both ambient and cold temperatures. During the deployments, the joints were stowed with the motor and then allowed to deploy, rotating the inertial simulator at the same time. These tests were used to determine deployment times and demonstrate that the joints would deploy at cold temperatures.

PHASE 3: BOOM ASSEMBLY TESTING

Deployment testing of the booms provides the remaining information necessary for the torque margin verification. Specifically, it is used to determine the cable harness bending torque, blanket bending torque, and bearing friction torque with all components in flight configuration. As explained earlier, a total of four booms and four reflectors have been built. All four booms will go through at least five deployments at ambient conditions. In addition, one boom will go through a series of protoflight tests, which include one cold and one hot thermal-vacuum deployment. Information obtained at temperature on the protoflight unit will be applied to the other units by similarity.

Boom deployment tests are run on a large aluminum frame that holds the inner boom arm fixed (Figure 8). A spacecraft simulator is attached to the shoulder and is supported by a cable running from a point on the ceiling directly above the shoulder pivot axis to a point on the spacecraft simulator. This cable forms a conical pendulum that offloads the weight of the spacecraft simulator as it deploys about the shoulder axis. The spacecraft simulator has the same inertia about the shoulder axis as the boom and reflector assembly and it also has all of the spacecraft interface attachment points.

A second cable goes from the wrist to a point on the ceiling directly above the elbow. This cable forms a conical pendulum which allows the outer arm to deploy about the elbow axis. The wrist axis is perpendicular to the shoulder and elbow axes. Deployment about the wrist axis requires a counterweight that places the mass center of all parts outboard of the wrist on the wrist axis. Both offload cables have load cells in-line that monitor the loads in the cables during deployment. Having these load cells proved to be very valuable when diagnosing an alignment problem that will be discussed later.

Strain gages, mounted on a shaft coupled to the damper, are used to measure torque input to the dampers during deployment. Assuming that the joints deploy at a relatively constant rate, the torque input to the damper is equal to the spring torque minus any losses. Therefore losses due to cable harnesses, blanket bending and other non-damper-related losses can be determined by taking the difference between the spring drive torque determined during joint component testing, and the damper drive torque determined during boom deployment tests.

Figure 9 shows a typical damper torque vs. angle curve obtained during deployment testing. Superimposed on the graph are the spring torque results from the joint component test for the particular joint. The difference between the spring torque and the torque from the boom deployment test can be determined as shown in Figure 9. This difference is the total frictional loss of the joint during ambient deployment. It includes blanket friction, cable harness drag, bearing friction, latch friction, as well as test equipment influences. Damper friction and spring friction torques from component testing are added to this resistance to get the total resistive torque.

Three of the booms have completed pre-environmental deployment testing. One more boom will be tested pre-environmental and then all four will be re-tested after vibration and thermal cycling tests. Thermal-vacuum testing of the protoflight boom is scheduled for March, 1994. After the thermal-vacuum tests are conducted, a new total resistive torque value will be determined at cold temperature for one of the booms. This resistive torque will be compared with the ambient torques for that boom to determine what increase in torque was caused by the cold temperature. The resistive torques for the other three booms will then be increased by the same amount to determine their worst case torque margins by similarity.

Boom deployment tests are run on a large aluminum frame that holds the inner boom arm fixed (Figure 8). A spacecraft simulator is attached to the shoulder and is supported by a cable running from a point on the ceiling directly above the shoulder pivot axis to a point on the spacecraft simulator. This cable forms a conical pendulum that offloads the weight of the spacecraft simulator as it deploys about the shoulder axis. The spacecraft simulator has the same inertia about the shoulder axis as the boom and reflector assembly and it also has all of the spacecraft interface attachment points.

A second cable goes from the wrist to a point on the ceiling directly above the elbow. This cable forms a conical pendulum which allows the outer arm to deploy about the elbow axis. The wrist axis is perpendicular to the shoulder and elbow axes. Deployment about the wrist axis requires a counterweight that places the mass center of all parts outboard of the wrist on the wrist axis. Both offload cables have load cells in-line that monitor the loads in the cables during deployment. Having these load cells proved to be very valuable when diagnosing an alignment problem that will be discussed later.

Strain gages, mounted on a shaft coupled to the damper, are used to measure torque input to the dampers during deployment. Assuming that the joints deploy at a relatively constant rate, the torque input to the damper is equal to the spring torque minus any losses. Therefore losses due to cable harnesses, blanket bending and other non-damper-related losses can be determined by taking the difference between the spring drive torque determined during joint component testing, and the damper drive torque determined during boom deployment tests.

Figure 9 shows a typical damper torque vs. angle curve obtained during deployment testing. Superimposed on the graph are the spring torque results from the joint component test for the particular joint. The difference between the spring torque and the torque from the boom deployment test can be determined as shown in Figure 9. This difference is the total frictional loss of the joint during ambient deployment. It includes blanket friction, cable harness drag, bearing friction, latch friction, as well as test equipment influences. Damper friction and spring friction torques from component testing are added to this resistance to get the total resistive torque.

Three of the booms have completed pre-environmental deployment testing. One more boom will be tested pre-environmental and then all four will be re-tested after vibration and thermal cycling tests. Thermal-vacuum testing of the protoflight boom is scheduled for March, 1994. After the thermal-vacuum tests are conducted, a new total resistive torque value will be determined at cold temperature for one of the booms. This resistive torque will be compared with the ambient torques for that boom to determine what increase in torque was caused by the cold temperature. The resistive torques for the other three booms will then be increased by the same amount to determine their worst case torque margins by similarity.

SECTION 3: LOAD ABSORBER DESIGN DEVELOPMENT

The MSAT Load Absorber has proven to be an effective way to dissipate unfurling energy for the MSAT reflectors. It is a non-viscous energy dissipating mechanism with potential applications in other systems requiring low-weight, non-velocity dependent, and high energy dissipating capability. The next section of this paper will discuss the design characteristics of the Load Absorber, describe the key Load Absorber lessons learned, and present the current acceptance and qualification test status of the Load Absorbers.

LOAD ABSORBER DESIGN

The need for the Load Absorber arose after a development boom and reflector had already been built and the four end-items units were in assembly. During testing of the development reflector, it was determined that the reflector would need to be redesigned to stiffen the ribs allowing the reflector to maintain shape after deployment in 1 g. Stiffening the ribs resulted in increased predicted deployment energy, producing lock-up loads on the spacecraft and boom which were much higher than allowed. It was the need to reduce the loads that led to the implementation of the Load Absorber in parallel with the redesign of the reflector.

The following were the key design drivers for the load absorber:

- 1) Implementation late in the program required quick development, incorporation within existing envelopes, and mating to existing hardware.
- 2) Complicated force coupling required that the force profile be well defined, weight be minimized, and variability in force be minimized.
- 3) Maximum reflector unfurling energy must be known to avoid bottoming out against the boom structure and the resulting high forces.
- 4) To ensure reflector rib lockup, the force reaction had to exceed 17 N-m for a minimum of 1 second.
- 5) All boom mechanism requirements were to be met, including 175% torque margin for the return springs.
- 6) Alignment and positional repeatability errors had to be minimized so as not to significantly increase the overall pointing error for the assembly.

These requirements were met by adding an energy-absorbing mechanism called a Load Absorber at the end of the boom near the reflector hub. A key aspect of the Load Absorber is how the reflector rotational motion is converted to axial motion. During unfurling of the reflector, a torsional loading is applied to the the Load Absorber interface plate (See Figure 4). The interface plate is connected to the boom through a duplex-ball-bearing interface that allows the plate to pivot about the bearing axis. As the interface plate rotates, the torsional load is converted to axial loading on the Megatube honeycomb assembly through a high-strength stainless steel band operating on a constant radius cam. The kinetic energy associated with the unfurling is dissipated by the linear crushing of the honeycomb. After the honeycomb has been crushed, a constant-torque spring returns the Load Absorber to its original configuration. The return spring also

provides sufficient preload of the load absorber to maintain pointing accuracy, even with the specified on-orbit spacecraft excitations.

Initially, the Load Absorber had only one cylinder of honeycomb producing a single reaction load level during reflector deployment. The honeycomb crush strength and stroke were sized to absorb the estimated deployment energy from the stiffened end-item reflector. Because of the uncertainty in the estimates of the reflector energy, the initial end-item reflector deployment was performed with a stronger crush strength honeycomb. This was allowable since the test was not performed on the end-item boom. The energy absorbed by the stronger honeycomb in this test indicated that the reflector deployment energy would significantly exceed the energy absorption capability of the honeycomb intended for flight use.

In order to absorb the additional energy and still keep the loads transmitted to the boom and spacecraft acceptable, a longer, softer honeycomb was required. However, this conflicted with the minimum torque required to ensure reflector lockup. Therefore, the Load Absorber was redesigned to incorporate a two-stage honeycomb system. During the first approximately 15 degrees of Load Absorber rotation, (approximately 1 second of reflector unfurling), the crush strength was sufficient to lockup the reflector ribs. Following rib lockup, a low torque, long duration, energy dissipation phase was implemented. See Figure 10 for the design configuration and Figure 11 for the two-stage force profile. Note Figure 11 shows both a minimum and maximum crush force profile, the actual profile will lie in the working domain depending on the deployment energy.

In the two-stage design, the honeycomb is stacked in series such that initially both pieces of honeycomb are being crushed at the same time. A mechanical fuse is used to allow the two honeycomb phases to function together. Each piece of honeycomb is grounded to the Megatube, passing loads directly from the honeycomb to the support boom tube. When the phase I honeycomb (2.5 cm) reaches solid crush height, a fusible link is fractured and the phase II honeycomb continues crushing at its lower load level.

Both phases of honeycomb are contained within the Megatube assembly. This assembly is comprised of two tubular frames supported by a "T" bracket and an "L" bracket. The "T" bracket is the primary load path to the boom mating bolt interface. The "L" bracket has an axial degree of freedom along the tube to allow for thermal expansion and contraction of the aluminum tube on the graphite boom.

KEY LESSONS LEARNED

Development testing also indicated that the friction between the piston and the guide tube played a critical role in the repeatability of the load absorber assembly crush force. It was initially anticipated that the honeycomb would crush straight, with little tendency to deform in a bending mode. In actuality, the minor variation in position of the honeycomb relative to the band force caused a

significant side force between the piston and the tube. Several different lubricants were employed including dry films (moly-disulfide and Anotef) as well as moly grease, however, the magnitude and variability in the friction properties were not satisfactory. Therefore, low friction wheels employing ball bearings were incorporated into the piston assemblies for each phase of the honeycomb.

The mechanical fuse was selected as the simplest concept to connect the two honeycomb cylinders and provide the desired two-stage crush force profile. The fuse is a tensile specimen designed for ultimate failure; it is an aluminum part with a functional diameter of 0.318 cm and a working length of approximately 1.27 cm polished to an 8 micro-finish. Development testing of the fusible links demonstrated that by pretesting all fusible links to 2% yield prior to installation the ultimate failure load could be accurately predicted within 5%. The fusible links have 2335 N yield strength and an additional +98 N force is required for fracture.

Knowledge of the actual loads being reacted by the Load Absorber was critical in the development of the final design. To gain this information, the bands were instrumented with strain gages and calibrated to 5338 N. This calibration also served as a proof test of each band.

The need to implement the two-stage Load Absorber, with the associated schedule and weight impacts, indicate the criticality of having the design requirements accurately defined early. The fact that the Load Absorber design and reflector redesign were proceeding in parallel made it difficult to accurately determine the reflector unfurling energy. In this situation, more conservatism in the design of the initial Load Absorber would have been helpful.

LOAD ABSORBER STATUS

At this time, the Load Absorber design has been qualified; four end-item units have been built, acceptance tested, and are installed on the end-item booms. This process included a series of torque margin tests very similar to those described previously for the boom as well as functional tests (both ambient and thermal) to validate each Load Absorber meets the force profile shown in Figure 11.

In addition to these four flight units, a fifth flight-quality Load Absorber has been built and acceptance tested to support the deployment tests of the end-item reflectors. This unit has been tested during actual deployments of the flight reflectors in ambient and thermal-vacuum environments.

CONCLUSION AND SUMMARY

The plan behind the MSAT boom torque margin verification can be summarized by the following guidelines:

1. Identify and understand all parameters that will affect the torque margin as early as possible.
2. Involve test personnel early in the design process to ensure testability of the hardware.
3. When testing several units, emphasize making test equipment automated and data acquisition systems easy to program and use.
4. Thoroughly test all components before installation in assemblies to detect problems early. However, test in environmental conditions only the parameters that are expected to have significant impact.
5. Thoroughly analyze test fixtures to identify test equipment influences.

Each of these guidelines is intended to discover potential problems as early and make the testing as efficient as possible. For the most part these guidelines were successfully followed on the MSAT booms, with the most notable exception being the problems that occurred during boom deployment testing. These guidelines along with the lessons learned from the actual testing provide a good example that can be applied to many other types of spacecraft mechanisms.

The MSAT Load Absorber has proven to be an effective way to dissipate unfurling energy for the MSAT reflectors. The ability to create a complex load profile, using two stages of honeycomb and fusible link, has been effectively demonstrated. The lessons learned from the load absorber design and testing can be applied to other types of spacecraft mechanism requiring low weight, high energy dissipation.

ACKNOWLEDGMENTS

The authors would like to acknowledge Dave Putnam who was responsible for coordinating the design of the booms, as well as developing the testing strategy, and Darrell Shen whose effort made the Load Absorber possible. We would also like to thank Ed Boesiger for his editorial assistance.

REFERENCES

1. Ellis, R.C., Fink, R.A., Rich, R.W., "Eddy Current Damper", Proceedings of the 23rd Aerospace Mechanisms Symposium, May 1989, NASA Conference Publication 3032.

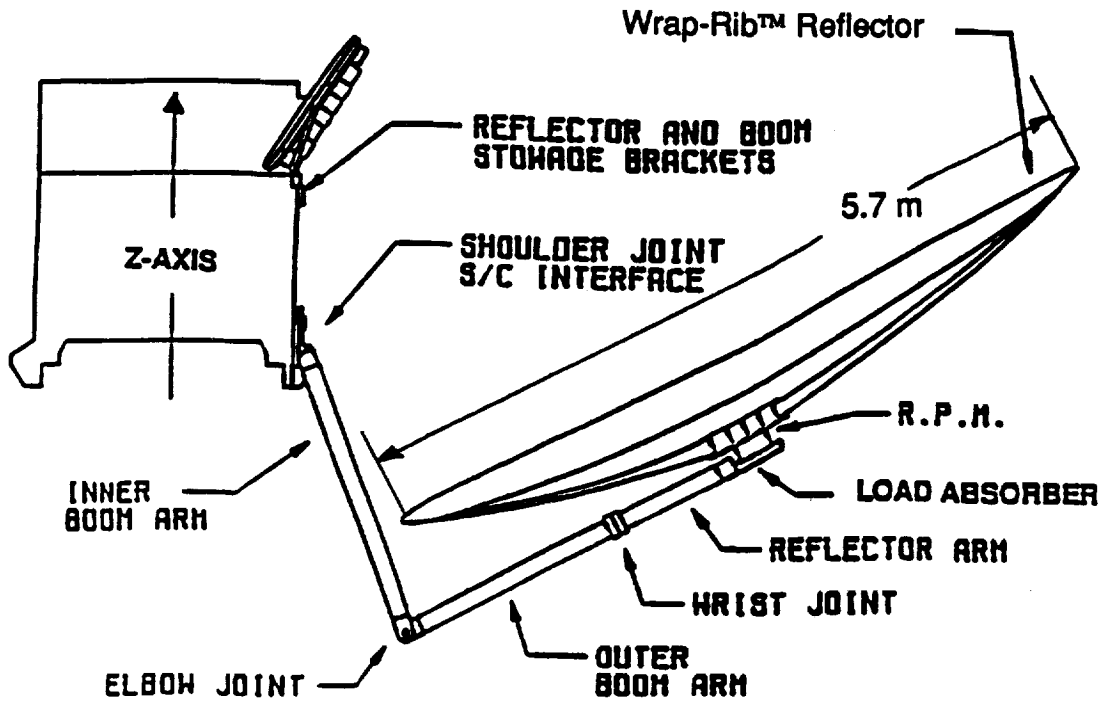


Figure 1. MSAT Reflector and Boom Deployed Configuration

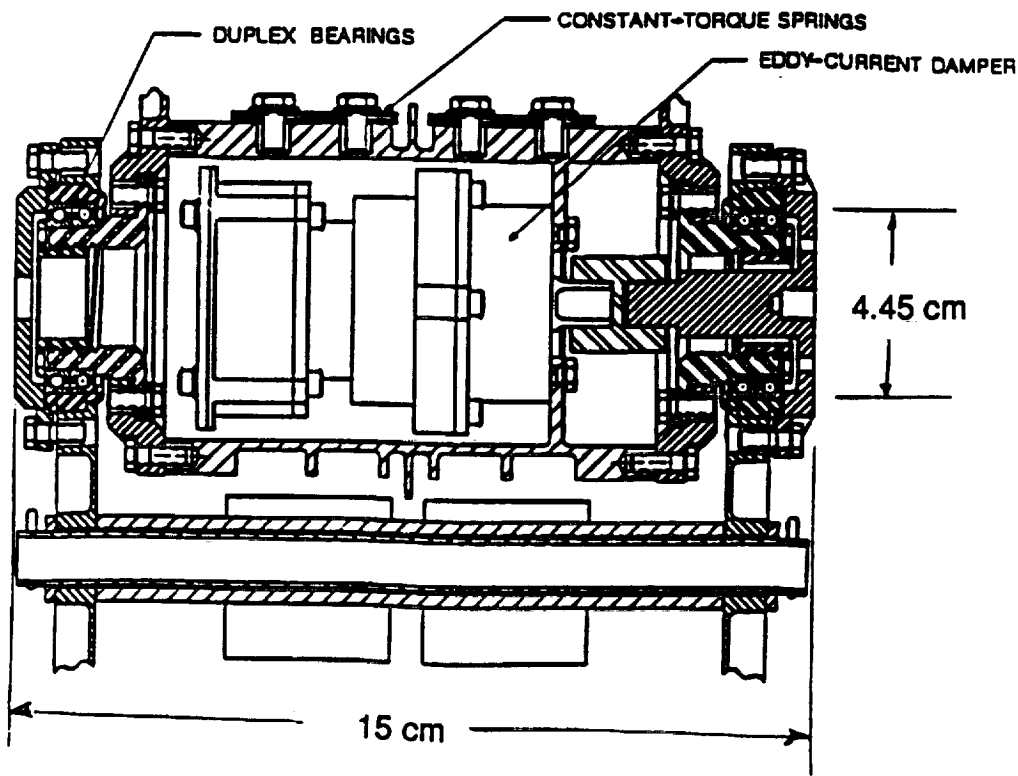


Figure 2. Wrist Joint Cross-section

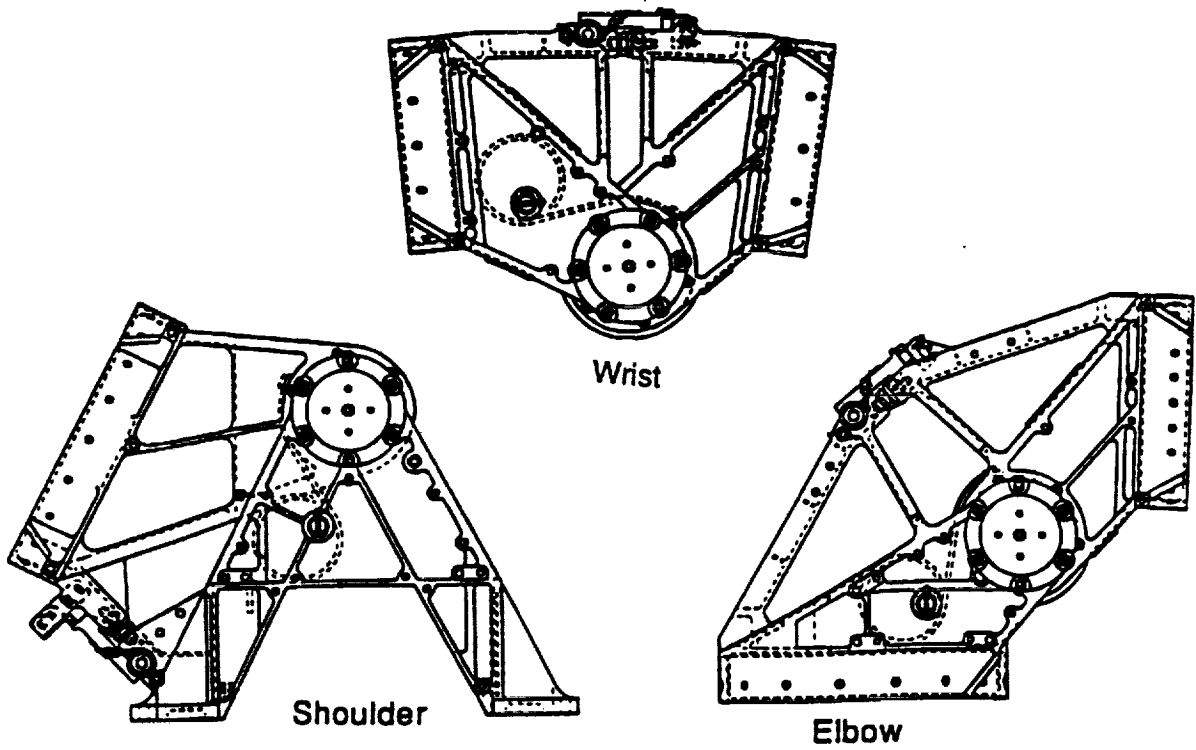


Figure 3. MSAT Boom Joints Deployed Configuration

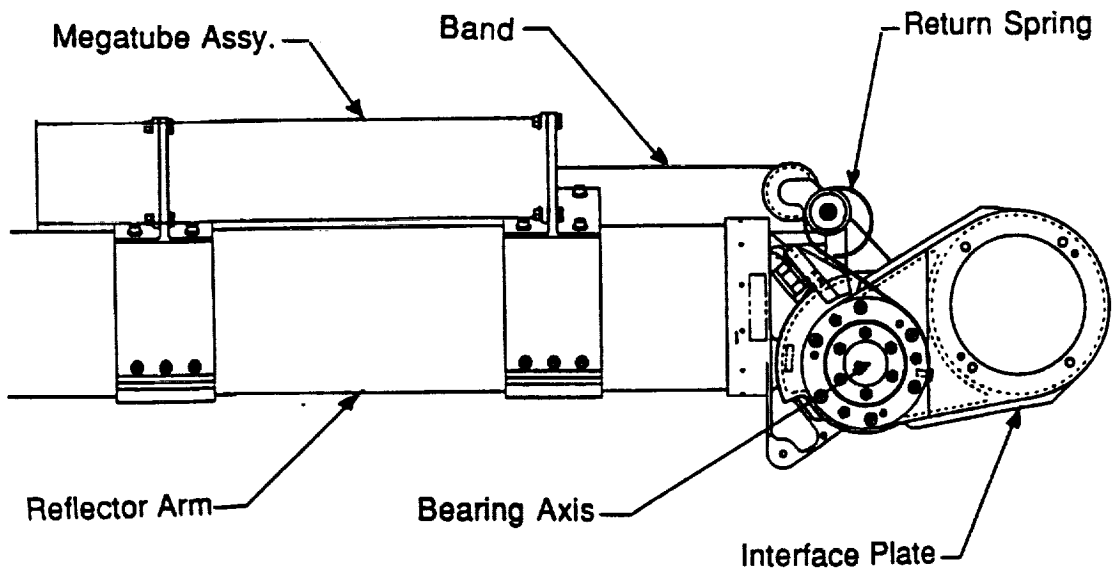


Figure 4. MSAT Load Absorber

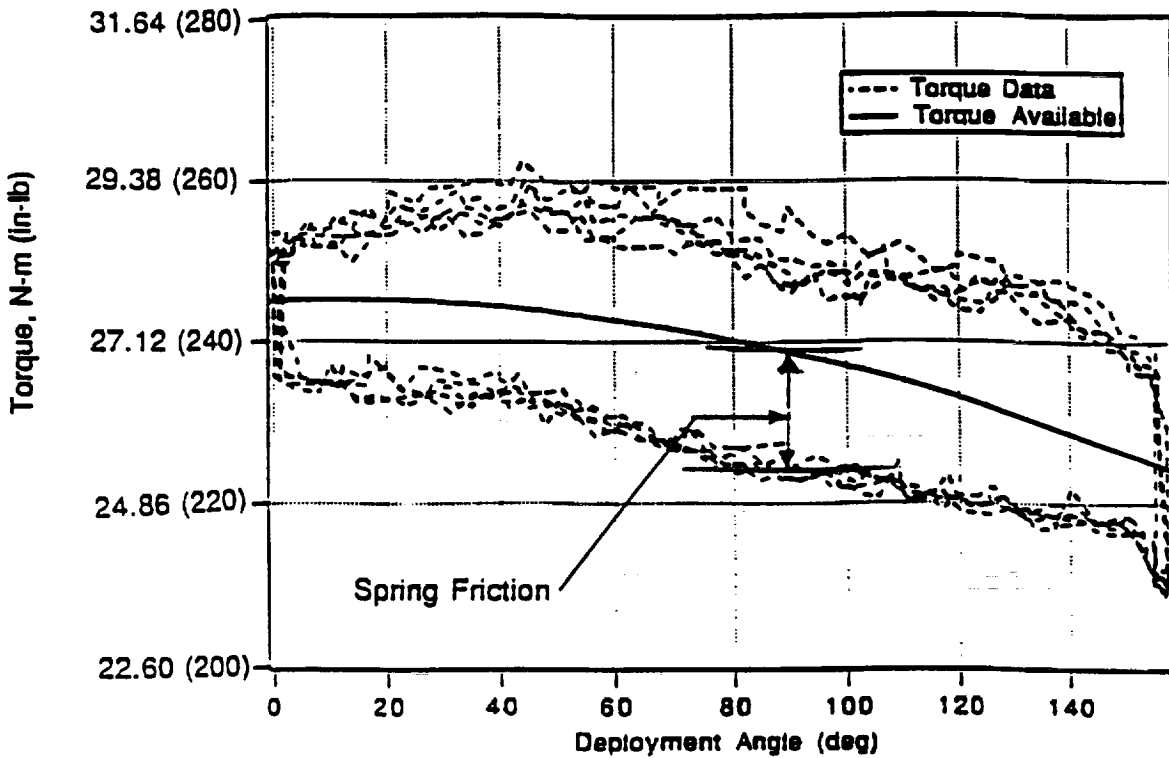


Figure 5. Shoulder Spring Torque vs. Deployment Angle Data from spring component testing

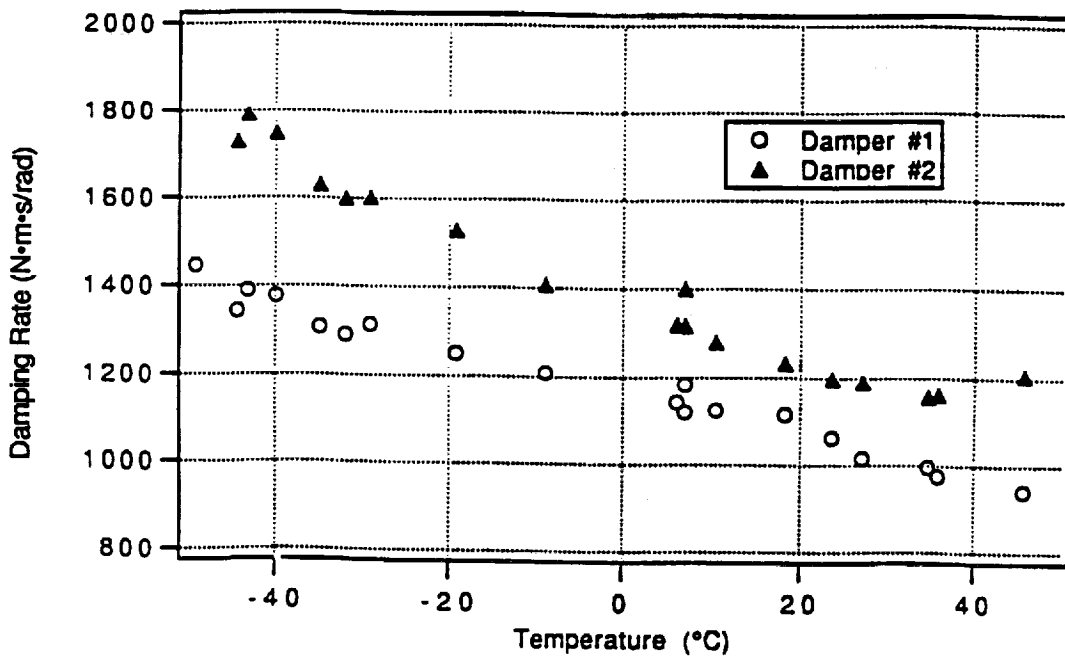


Figure 6. Damping Rate vs. Temperature for 2 Dampers Data from damper component testing.

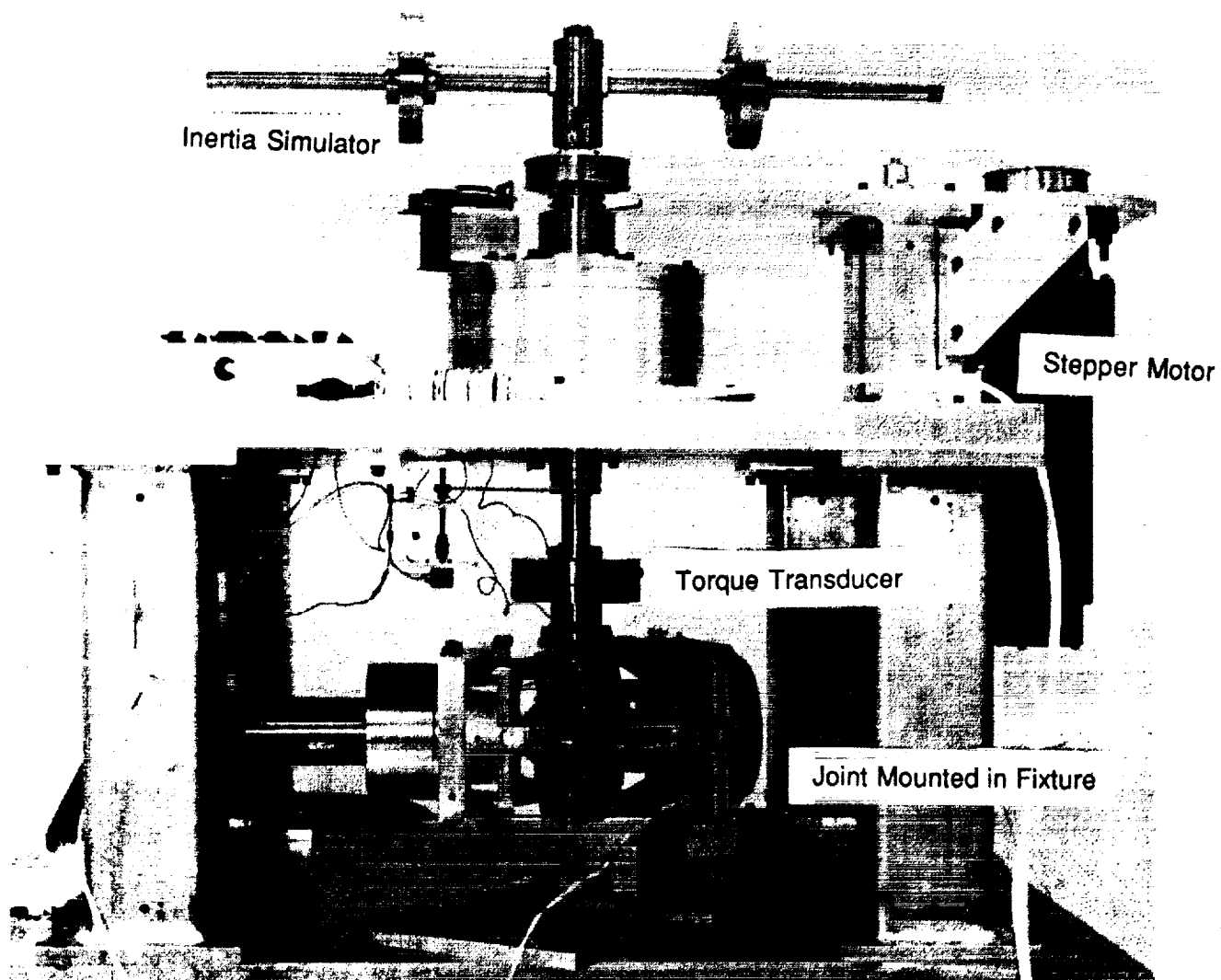


Figure 7. Joint Test Stand with Joint Installed

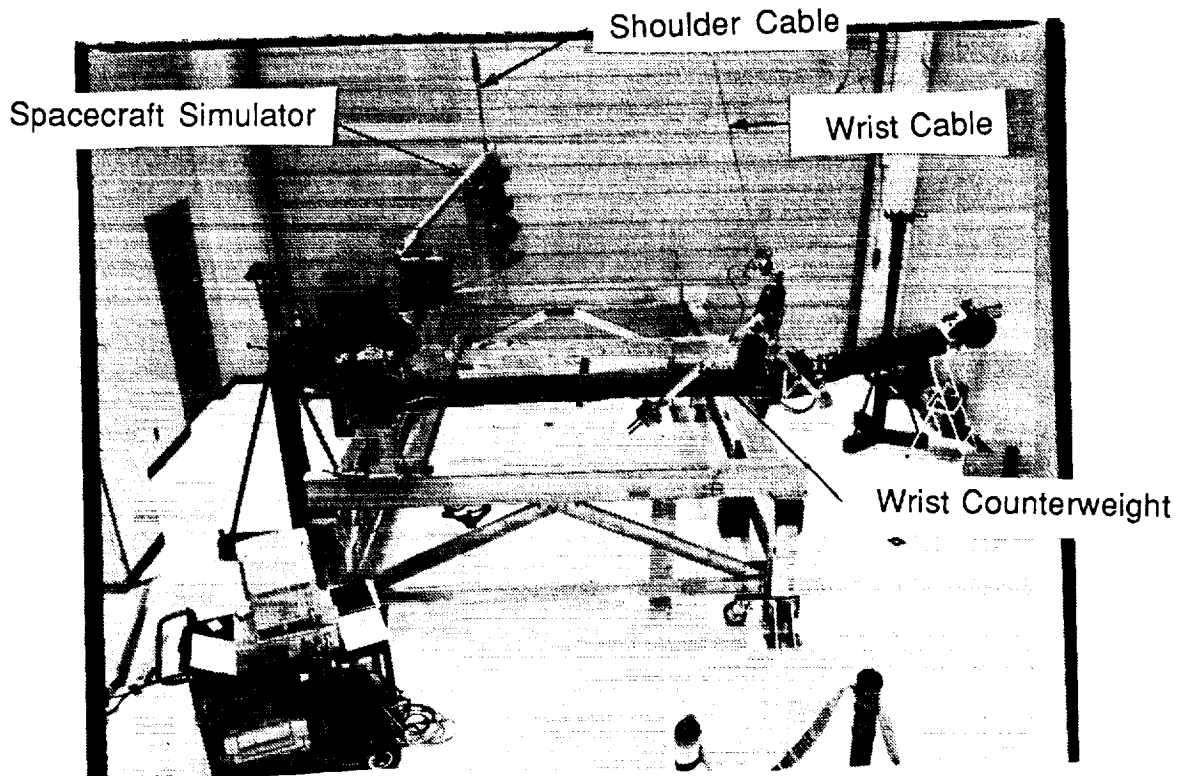


Figure 8. Boom Deployment Stand with Development Boom Installed

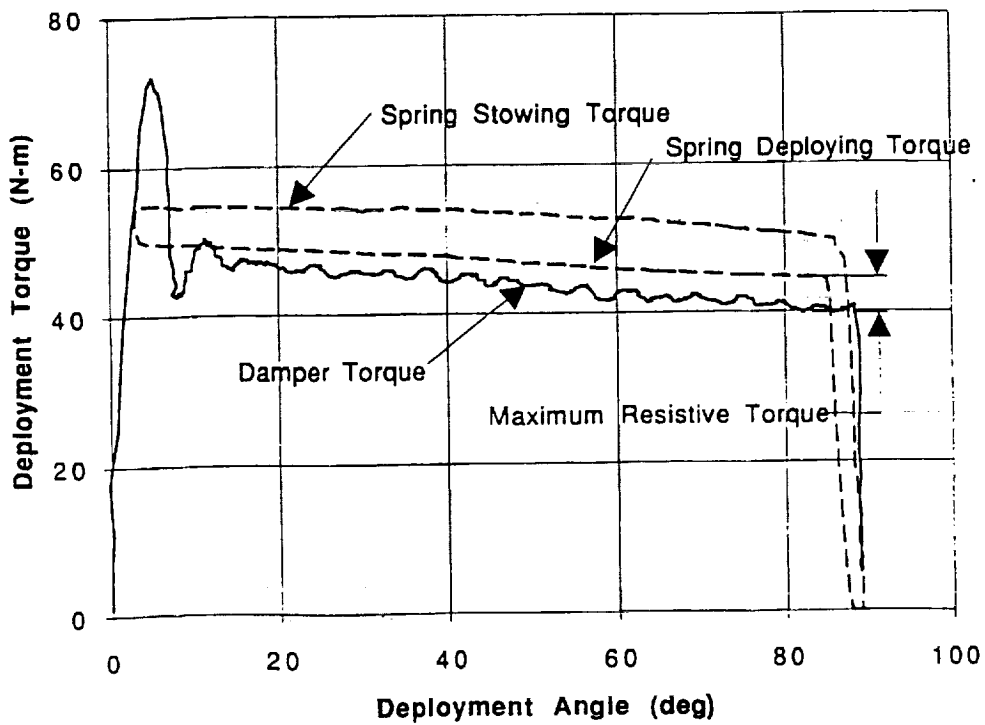


Figure 9. Damper and Spring Torque vs. Angle
 (Damper torque determined during boom deployment testing, spring torque determined during joint component testing)

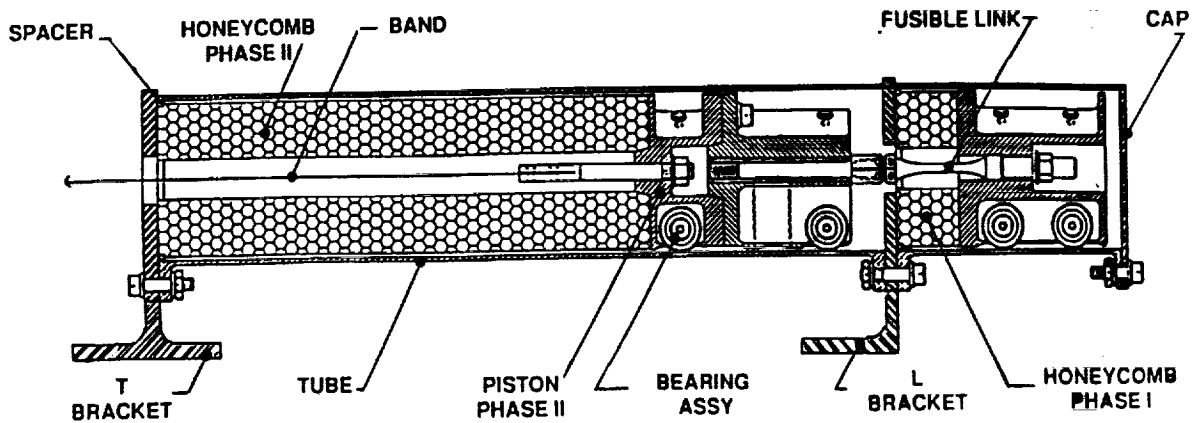


Figure 10. Load Absorber Megatube Assembly

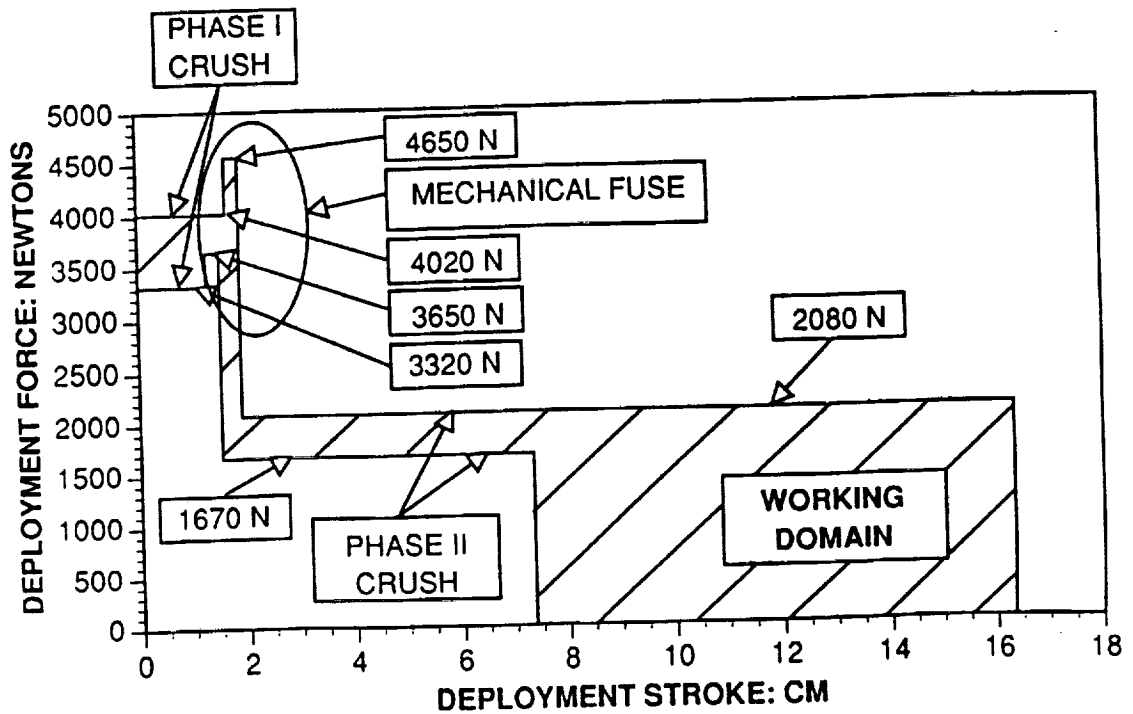


Figure 11. Load Absorber Force Profile
(Maximum and minimum profiles shown. Actual profile in working domain.)